Challenge Journal of Structural Mechanics

Research Article

Natural frequencies of porous orthotropic two-layered plates within the shear deformation theory

Ferruh Turan [a,*]

[a] *Department of Civil Engineering, Ondokuz Mayıs University, 55139 Samsun, Türkiye*

ABSTRACT

This paper analyzes the natural frequencies of porous orthotropic laminated composite plates with two different porosity models based on the higher-order shear deformation theory. The fundamental relations of natural frequency analysis are derived by using the virtual work principle and hyperbolical shear deformation theory. The obtained partial differential equations system is reduced to an ordinary differential equations system via approximation functions suitable for simply supported boundary conditions and the Galerkin method. After some mathematical operations, the natural frequency equation of porous orthotropic laminated composite plates is obtained in the framework of hyperbolical shear deformation theory. The natural frequency equation based on the classical laminated plate theory can be determined by ignoring the shear strains in the theoretical formulations. After two validation studies by using appropriate results in the literature, parametric analyses are performed to show the sensitivity of natural frequencies to shear deformation, porosity model, orthotropy, layer sequence, and geometric properties.

ARTICLE INFO

Article history:
Received 9 August 2022
Revised 2 November 2022
Accepted 18 November 2022

Keywords:
Porosity
Porous plate
Laminated composite
Vibration
Shear deformation
Orthotropy

1. Introduction

Structural elements in many industries such as aviation, maritime, automotive, and military are required to consist of lightweight materials with high strength, excellent energy absorption, and low thermal conductivity. The pores in the structural elements can also occur as micro-defects. Therefore, the sensitivity of structural responses such as stability and vibration frequency to micro-defects or pores needs to be analyzed in detail.

Zhou et al. (2020) analyzed the free vibration response of rectangular functionally graded plates with two different distributed interior pores and platelets of graphene. Zhong et al. (2021) investigated the in-plane vibration of porous circular plates with porosity distributions in thickness and radial directions. Teng and Xi (2021) examined the porosity effect on the free vibration and stability behavior of functionally graded rectangular plates. Pan et al. (2021) analyzed the free vibration problem of graphene-reinforced porous plates. Pham et al. (2021) investigated static and dynamic responses of functionally graded nano-plates with uneven and logarithmic-uneven porosity distributions. Esen and Özmen (2022) studied the thermal vibration and buckling responses of functionally graded nano-plates modeled by porosity distribution functions. Lahdiri and Kadri (2022) examined the effect of porosity distributions on the free vibration of the multi-directional functionally graded porous plates. Chen et al. (2022) investigated the free in-plane vibration response of functionally graded plates with porosity distributions in the thickness and in-plane directions.

Neglecting transverse shear deformations while investigating structural elements' static and dynamic responses leads to inaccurate results. Therefore, there is an increasing tendency for researchers to develop novel theories that include the effects of transverse shear deformations (Aydogdu 2009; Mahi et al. 2015; Shi et al. 2018). Depending on the development of novel shear deformations, articles have appeared in the literature on examining the static and dynamic responses of porous structure components within the scope of shear defor-

* *Corresponding author*. Tel.: +90-362-312-1919 ; Fax: +90-362-457-6091 ; E-mail address: ferruh.turan@omu.edu.tr (F. Turan)
ISSN: 2149-8024 / DOI: https://doi.org/10.20528/cjsmec.2023.01.001

mation theory. Arshid et al. (2020) investigated the static and dynamic behavior of functionally graded graphene-reinforced porous annular microplates based on first-order shear deformation theory. Li et al. (2020) analyzed the static and dynamic responses of porous bi-directional functionally graded plates within the first-order shear deformation theory. Kumar et al. (2021) examined the vibration frequencies of functionally graded porous nano-plates under the trigonometric shear deformation theory. Wang et al. (2022) investigated the vibration response of functionally graded circular plates modeled by the modified porous material power-law rule in the thermal environment within the first-order shear deformation theory. Kumar and Harsha (2022) analyzed the static and vibration behavior of sigmoid functionally graded piezoelectric plates with two porosity distributions under the first-order shear deformation theory. Hung et al. (2022) examined the free vibration and buckling behavior of porous micro-plates with three porosity distributions based on shear deformation theory.

Laminated composite plates can be more sensitive than conventional plates due to the disadvantages such as discontinuity between layers and weak shear strength. In addition, different orientation angles or layer stacks can also affect the structural performance of laminated composite plates. The laminated composite plates' static and dynamic responses were investigated using shear deformation theories (Reddy and Phan 1985; Fares and Zenkour 1999; Zenkour and Radwan 2016; Turan et al. 2017). Furthermore, it is necessary to analyze micro-defects and determine their effect on laminated composite plates' static and dynamic behavior. Yuan et al. (2019) analyzed the static problem of sandwich plates with three porosity distributions within first-order shear deformation theory. Xu et al. (2019) examined the influence of three different porosity distributions through the core thickness on the buckling of functionally graded porous cores sandwich plates under the shear deformation theory. Safaei (2020) studied the porosity effect on the free vibration frequencies of porous laminated composite sandwich plates based on the shear deformation theory. Esmaeilzadeh et al. (2020) examined the dynamic response of an axially moving two-layer porous laminated plate within the first-order shear deformation theory.

Porous materials are widely used today to reduce structural weight and manage vibration responses. On the other hand, laminated composites are other materials commonly used in industries such as automotive and aircraft due to their properties, such as strength/weight ratio. Accordingly, porous laminated composites are expected to be more advantageous than conventional laminated composite structures in terms of weight reduction, stiffness increase, and vibration response management. However, mechanical analyzes of such structures need to be carried out in detail. In addition, the literature review reveals that the free vibration problem of porous orthotropic two-layered plates has not yet been investigated. Therefore, this study is analyzed the natural vibration behavior of porous orthotropic layered plates. Two different porosity distributions and hyperbolic shear deformation theory are considered. The effects of porosity, shear deformation, orthotropy, layer arrangement, and geometric properties on the natural frequencies of porous orthotropic laminated plates are investigated.

2. Mathematical Model

Composite structures, known as two-layered porous structures, are produced by bonding two porous orthotropic layers to each other. In general, adopting porous composite structures can significantly reduce the system mass while maintaining the same level of stiffness. One of the most attractive applications for porous laminated composite structures is the prototype fabrication of high-speed trains. A porous orthotropic laminated composite plate with a length of edges a, b, and uniform thickness h is considered. Fig.1 presents a coordinate system $(\bar{x}, \bar{y}, \bar{z})$ in which the $(\bar{x}, \bar{y})$ plane is on the plate's mid-plane and $\bar{z}$ in the thickness direction. The angles $\theta_1, \theta_2, \ldots, \theta_N$ represents the layer orientation angle.

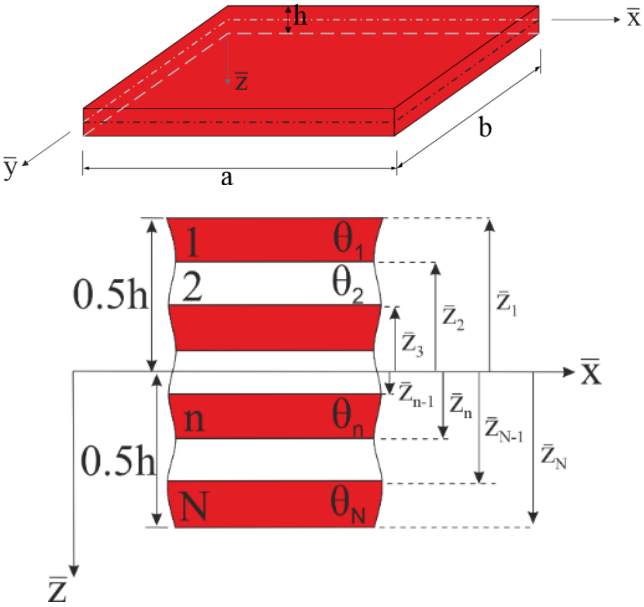

Fig. 1. Geometry, coordinate system and cross-section of a porous orthotropic laminated composite plate.

The material properties of porous materials are modeled by location's continuous function as two types of porosity model (pm). Eq. (1) determine the porous material properties.

$$El_{11}^{(n)}(z) = El_{01}^{(n)}\left(1 - kf^{(n)}(z)\right)$$

$$El_{22}^{(n)}(z) = El_{02}^{(n)}\left(1 - kf^{(n)}(z)\right)$$

$$Sh_{12}^{(n)}(z) = Sh_{012}^{(n)}\left(1 - kf^{(n)}(z)\right)$$

$$Sh_{13}^{(n)}(z) = Sh_{013}^{(n)}\left(1 - kf^{(n)}(z)\right)$$

$$Sh_{23}^{(n)}(z) = Sh_{023}^{(n)}\left(1 - kf^{(n)}(z)\right)$$

$$\rho^{(n)}(z) = \rho_0^{(n)}\left(1 - kf^{(n)}(z)\right)$$

$$n = 1,2,..,N, z = \bar{z}/h \quad (1)$$

where $El_{01}^{(n)}$ and $El_{02}^{(n)}$ are the Young's modulus of the non-porous material in the $\bar{x}$ and $\bar{y}$ directions, and $\rho_0^{(n)}$ is the mass density of the non-porous material. $Sh_{012}^{(n)}$, $Sh_{013}^{(n)}$, and $Sh_{023}^{(n)}$ are the shear modulus of the non-porous orthotropic material in the $\bar{x}\bar{y}$, $\bar{x}\bar{z}$, and $\bar{y}\bar{z}$ planes, respectively. k is the porosity coefficient and the condition $0 \leq k < 1$ is satisfied. Also, $k = 0$ corresponds to the non-porous orthotropic material (pm_1). $f^{(n)}(z)$ is the porosity distribution function of the *n*nt layer and is defined as:

$$f^{(n)}(z) = \begin{cases} \cos(\pi z), pm_2 \\ \frac{3.45}{\pi}\sin(\pi z), pm_3 \end{cases} \quad (2)$$

Fig. 2 presents the porosity models' graphical representation for the $El_{11}(z)$ function.

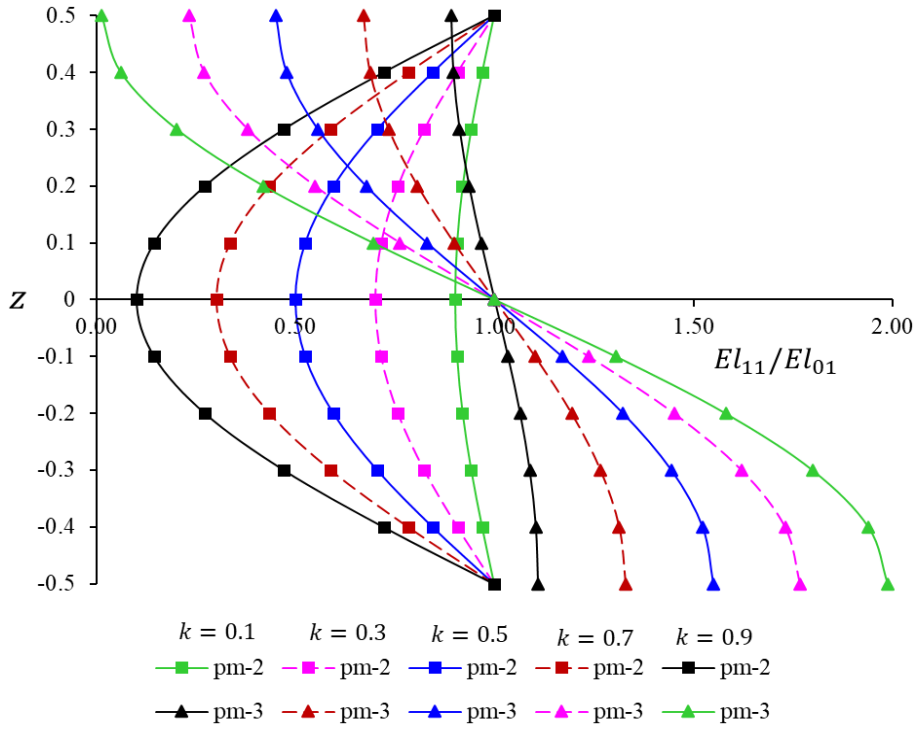

Fig. 2. Graphical representation of the porosity models for the $El_{11}(z)$ function.

3. Governing Equations

The governing equations are derived by using hyperbolical shear deformation theory in this study. The stress-strain relations of the nth porous orthotropic layer are (Reddy and Phan 1985; Fares and Zenkour 1999; Turan et al. 2017).

$$\begin{Bmatrix} \sigma_{\bar{x}} \\ \sigma_{\bar{y}} \\ \sigma_{\bar{y}\bar{z}} \\ \sigma_{\bar{x}\bar{z}} \\ \sigma_{\bar{x}\bar{y}} \end{Bmatrix}^{(n)} = \begin{bmatrix} d_{11} & d_{12} & 0 & 0 & d_{16} \\ d_{21} & d_{22} & 0 & 0 & d_{26} \\ 0 & 0 & d_{44} & d_{45} & 0 \\ 0 & 0 & d_{45} & d_{55} & 0 \\ d_{16} & d_{26} & 0 & 0 & d_{66} \end{bmatrix}^{(n)} \begin{Bmatrix} \varepsilon_{\bar{x}} \\ \varepsilon_{\bar{y}} \\ \varepsilon_{\bar{y}\bar{z}} \\ \varepsilon_{\bar{x}\bar{z}} \\ \varepsilon_{\bar{x}\bar{y}} \end{Bmatrix} \quad (3)$$

where $\varepsilon_{\bar{x}}$ and $\varepsilon_{\bar{y}}$ are strains in the $\bar{x}$ and $\bar{y}$ directions, $\varepsilon_{\bar{x}\bar{y}}$, $\varepsilon_{\bar{x}\bar{z}}$, $\varepsilon_{\bar{y}\bar{z}}$ are shear strains on the planes $\bar{x}\bar{y}$, $\bar{x}\bar{z}$, $\bar{y}\bar{z}$, respectively, and $d_{ij}^{(n)}(i,j = 1,2,..,6)$are the transformed material properties of the nth porous orthotropic layer given by (Zenkour and Radwan 2016; Turan et al. 2017)

$$d_{11} = e_{11}c^4 + e_{22}s^4 + 2(e_{12} + 2e_{66})s^2c^2, d_{12} = (e_{11} + e_{22} - 4e_{66})s^2c^2 + e_{12}(s^4 + c^4)$$

$$d_{16} = (e_{11} - e_{12} - 2e_{66})sc^3 + (e_{12} - e_{22} + 2e_{66})s^3c, d_{22} = e_{11}s^4 + e_{22}c^4 + 2(e_{12} + 2e_{66})s^2c^2$$

$$d_{26} = (e_{11} - e_{12} - 2e_{66})cs^3 + (e_{12} - e_{22} + 2e_{66})c^3s, d_{66} = (e_{11} + e_{22} - 2e_{12} - 2e_{66})c^2s^2 + e_{66}(s^4 + c^4)$$

$$d_{44} = e_{44}c^2 + e_{55}s^2, d_{45} = (e_{55} - e_{44})cs, d_{55} = e_{44}s^2 + e_{55}c^2$$

$$s = \sin\theta\,,\ c = \cos\theta \quad (4)$$

where θ is the angle between the global and local $\bar{x}$ −axes. $e_{ij}^{(n)}(i,j = 1,2,..,6)$ are the material properties of the n^{th} porous orthotropic layer defined as

$$e_{11}^{(n)}(z) = \frac{El_{11}^{(n)}(z)}{1-\upsilon_{12}^{(n)}\upsilon_{21}^{(n)}}, e_{12}^{(n)}(z) = \frac{\upsilon_{12}^{(n)}El_{22}^{(n)}(z)}{1-\upsilon_{12}^{(n)}\upsilon_{21}^{(n)}}, e_{21}^{(n)}(z) = \frac{\upsilon_{21}^{(n)}El_{11}^{(n)}(z)}{1-\upsilon_{12}^{(n)}\upsilon_{21}^{(n)}}$$

$$e_{22}^{(n)}(z) = \frac{El_{22}^{(n)}(z)}{1-\upsilon_{12}^{(n)}\upsilon_{21}^{(n)}}, e_{44}^{(n)}(z) = Sh_{23}^{(n)}(z), e_{55}^{(n)}(z) = Sh_{13}^{(n)}(z), e_{66}^{(n)}(z) = Sh_{12}^{(n)}(z)$$

$$z = \bar{z}/h, n = 1,2,..,N \quad (5)$$

where υ_{12} and υ_{21} are the Poisson ratios of the porous orthotropic layers and are assumed to be constant.

The porous orthotropic laminated composite plates' force and moment resultants based on the hyperbolical shear deformation theory are determined as:

$$\begin{aligned}
&\left(N_{\bar{x}}, N_{\bar{y}}, N_{\bar{x}\bar{y}}, M_{\bar{x}}, M_{\bar{y}}, M_{\bar{x}\bar{y}}\right) \\
&\quad = \sum_{n=1}^{N} \int_{\bar{z}_{n-1}}^{\bar{z}_n} \left(\sigma_{\bar{x}}^{(n)}, \sigma_{\bar{y}}^{(n)}, \sigma_{\bar{x}\bar{y}}^{(n)}, \bar{z}\sigma_{\bar{x}}^{(n)}, \bar{z}\sigma_{\bar{y}}^{(n)}, \bar{z}\sigma_{\bar{x}\bar{y}}^{(n)}\right) d\bar{z} \\
&\left(S_{\bar{x}}, S_{\bar{y}}, S_{\bar{x}\bar{y}}\right) \\
&\quad = \sum_{n=1}^{N} \int_{\bar{z}_{n-1}}^{\bar{z}_n} \left(\varphi(\bar{z})\sigma_{\bar{x}}^{(n)}, \varphi(\bar{z})\sigma_{\bar{y}}^{(n)}, \varphi(\bar{z})\sigma_{\bar{x}\bar{y}}^{(n)}\right) d\bar{z} \\
&\left(Q_{\bar{x}}, Q_{\bar{y}}\right) = \sum_{n=1}^{N} \int_{\bar{z}_{n-1}}^{\bar{z}_n} \left(\frac{d\varphi(\bar{z})}{d\bar{z}}\sigma_{\bar{x}\bar{z}}^{(n)}, \frac{d\varphi(\bar{z})}{d\bar{z}}\sigma_{\bar{y}\bar{z}}^{(n)}\right) d\bar{z}
\end{aligned} \tag{6}$$

where N, M, Q, and Srepresent force, moment, transverse shear force, and higher-order force components, respectively. Substituting Eq. (3) into Eq. (6) and then substituting the results into the virtual work principle yields

$$\begin{aligned}
&(\mathfrak{I}_{11}^0 + \mathfrak{I}_{22}^0 - 2\mathfrak{I}_{66}^0)\frac{\partial^4\gamma}{\partial\bar{x}\partial\bar{y}} + \mathfrak{I}_{21}^0\frac{\partial^4\gamma}{\partial\bar{y}^4} + \mathfrak{I}_{12}^0\frac{\partial^4\gamma}{\partial\bar{x}^4} + \mathfrak{I}_{11}^1\frac{\partial^4 w}{\partial\bar{x}^4} \\
&\quad + (\mathfrak{I}_{12}^1 + \mathfrak{I}_{21}^1 + 2\mathfrak{I}_{66}^1)\frac{\partial^4 w}{\partial\bar{x}^2\partial\bar{y}^2} + \mathfrak{I}_{22}^1\frac{\partial^4 w}{\partial\bar{y}^4} + \mathfrak{I}_{11}^2\frac{\partial^3\phi_1}{\partial\bar{x}^3} \\
&\quad + (\mathfrak{I}_{21}^2 + 2\mathfrak{I}_{66}^2)\frac{\partial^3\phi_1}{\partial\bar{x}\partial\bar{y}^2} + (\mathfrak{I}_{12}^2 + 2\mathfrak{I}_{66}^2)\frac{\partial^3\phi_2}{\partial\bar{x}^2\partial\bar{y}} + \mathfrak{I}_{22}^2\frac{\partial^3\phi_2}{\partial\bar{y}^3} \\
&\quad = \bar{\imath}_1\left(\frac{\partial^4 w}{\partial\bar{x}^2\partial t^2} + \frac{\partial^4 w}{\partial t^2\partial\bar{y}^2}\right) + \bar{\imath}_2\left(\frac{\partial^3\phi_1}{\partial\bar{x}\partial t^2} + \frac{\partial^3\phi_2}{\partial t^2\partial\bar{y}}\right) + \imath_0\frac{\partial^2 w}{\partial t^2}
\end{aligned} \tag{7a}$$

$$\begin{aligned}
&(\mathfrak{I}_{11}^3 - \mathfrak{I}_{66}^3)\frac{\partial^4\gamma}{\partial\bar{x}^2\partial\bar{y}^2} + \mathfrak{I}_{12}^3\frac{\partial^4\gamma}{\partial\bar{x}^4} + \mathfrak{I}_{11}^4\frac{\partial^4 w}{\partial\bar{x}^4} + \\
&\quad + (\mathfrak{I}_{12}^4 + \mathfrak{I}_{66}^4)\frac{\partial^4 w}{\partial\bar{x}^2\partial\bar{y}^2} + \mathfrak{I}_{11}^5\frac{\partial^3\phi_1}{\partial\bar{x}^3} + \mathfrak{I}_{66}^5\frac{\partial^3\phi_1}{\partial\bar{x}\partial\bar{y}^2} \\
&\quad + (\mathfrak{I}_{12}^5 + \mathfrak{I}_{66}^5)\frac{\partial^3\phi_2}{\partial\bar{x}^2\partial\bar{y}} - \tilde{d}_{55}^0\frac{\partial\phi_1}{\partial\bar{x}} \\
&\quad = -\bar{\imath}_2\frac{\partial^4 w}{\partial\bar{x}^2\partial t^2} + \bar{\imath}_3\frac{\partial^3\phi_1}{\partial\bar{x}\partial t^2}
\end{aligned} \tag{7b}$$

$$\begin{aligned}
&\mathfrak{I}_{21}^3\frac{\partial^4\gamma}{\partial\bar{y}^4} + (\mathfrak{I}_{22}^3 - \mathfrak{I}_{66}^3)\frac{\partial^4\gamma}{\partial\bar{x}^2\partial\bar{y}^2} + (\mathfrak{I}_{21}^4 + \mathfrak{I}_{66}^4)\frac{\partial^4 w}{\partial\bar{x}^2\partial\bar{y}^2} \\
&\quad + \mathfrak{I}_{22}^4\frac{\partial^4 w}{\partial\bar{y}^4} + (\mathfrak{I}_{21}^5 + \mathfrak{I}_{66}^5)\frac{\partial^3\phi_1}{\partial\bar{x}\partial\bar{y}^2} + \mathfrak{I}_{22}^5\frac{\partial^3\phi_2}{\partial\bar{y}^3} + \mathfrak{I}_{66}^5\frac{\partial^3\phi_2}{\partial\bar{x}^2\partial\bar{y}} \\
&\quad - \tilde{d}_{44}^0\frac{\partial\phi_2}{\partial\bar{y}} = -\bar{\imath}_2\frac{\partial^4 w}{\partial\bar{y}^2\partial t^2} + \bar{\imath}_3\frac{\partial^3\phi_2}{\partial\bar{y}\partial t^2}
\end{aligned} \tag{7c}$$

in which the terms may be found in Appendix A. $\gamma(\bar{x}, \bar{y}, t)$ is the Airy stress function. The compatibility equation for the porous orthotropic laminated composite plate can be written as

$$\begin{aligned}
&\tau_{11}^0\frac{\partial^4\gamma}{\partial\bar{y}^4} + (\tau_{12}^0 + \tau_{21}^0 + \tau_{66}^0)\frac{\partial^4\gamma}{\partial\bar{x}^2\partial\bar{y}^2} + \tau_{22}^0\frac{\partial^4\gamma}{\partial\bar{x}^4} \\
&\quad + (\tau_{11}^1 + \tau_{22}^1 - \tau_{66}^1)\frac{\partial^4 w}{\partial\bar{x}^2\partial\bar{y}^2} + \tau_{12}^1\frac{\partial^4 w}{\partial\bar{y}^4} + \tau_{21}^1\frac{\partial^4 w}{\partial\bar{x}^4} \\
&\quad + (\tau_{11}^3 - \tau_{66}^3)\frac{\partial^3\phi_1}{\partial\bar{x}\partial\bar{y}^2} + (\tau_{22}^3 - \tau_{66}^3)\frac{\partial^3\phi_2}{\partial\bar{x}^2\partial\bar{y}} + \tau_{21}^3\frac{\partial^3\phi_1}{\partial\bar{x}^3} \\
&\quad + \tau_{12}^3\frac{\partial^3\phi_2}{\partial\bar{y}^3} = 0
\end{aligned} \tag{8}$$

The porous orthotropic laminated composite plates' natural frequencies are determined with Eqs. (7) and (8).

4. Solution Procedure

Consider a simply supported porous orthotropic laminated composite plate whose boundary conditions are as follows:

$$\begin{aligned}
&v_0 = w = \phi_2 = M_{\bar{x}} = 0, \text{at } \bar{x} = 0, a \\
&u_0 = w = \phi_1 = M_{\bar{y}} = 0, \text{at } \bar{y} = 0, b
\end{aligned} \tag{9}$$

Based on the boundary conditions (9), the approximate solutions can be represented by

$$\begin{aligned}
&w(\bar{x}, \bar{y}, t) = \tilde{w}(t)\sin(\eta_1\bar{x})\sin(\eta_2\bar{y}) \\
&\phi_1(\bar{x}, \bar{y}, t) = \tilde{\phi}_1(t)\cos(\eta_1\bar{x})\sin(\eta_2\bar{y}) \\
&\phi_2(\bar{x}, \bar{y}, t) = \tilde{\phi}_2(t)\sin(\eta_1\bar{x})\cos(\eta_2\bar{y}) \\
&\eta_1 = \frac{m_1\pi}{a}, \quad \eta_2 = \frac{m_2\pi}{b}
\end{aligned} \tag{10}$$

where $\tilde{w}(t), \tilde{\phi}_1(t), \tilde{\phi}_2(t)$ are the time dependent coefficients and m_1,m_2 are the numbers of half waves.

By substituting Eq. (10) into the compatibility Eq. (8) and solving obtained equation for unknown γ leads to

$$\begin{aligned}
&\gamma(x, y, t) = \left(\tilde{w}(t)\beta_1 + \tilde{\phi}_1(t)\beta_2 + \right. \\
&\left.\tilde{\phi}_2(t)\beta_3\right)\sin(\eta_1\bar{x})\sin(\eta_2\bar{y})
\end{aligned} \tag{11}$$

with

$$\begin{aligned}
&\beta_1 = -\frac{\eta_1^4\tau_{21}^1 + \eta_1^2\eta_2^2(\tau_{11}^1 + \tau_{22}^1 - \tau_{66}^1) + \eta_2^2\tau_{12}^1}{\alpha} \\
&\beta_2 = -\frac{\eta_1\eta_2^2(\tau_{11}^3 - \tau_{66}^3) + \eta_1^3\tau_{21}^3}{\alpha} \\
&\beta_3 = -\frac{\eta_1^2\eta_2(\tau_{22}^3 - \tau_{66}^3) + \eta_1^3\tau_{12}^3}{\alpha} \\
&\alpha = \eta_1^4\tau_{22}^0 + \eta_1^2\eta_2^2(\tau_{12}^0 + \tau_{21}^0 + \tau_{66}^0) + \eta_2^4\tau_{11}^0
\end{aligned} \tag{12}$$

Replacing Eqs. (10) and (11) into Eqs. (7a), (7b), and (7c) and then applying Galerkin method to the resulting equations yields

$$\begin{aligned}
&\ell_{11}\frac{d^2\tilde{w}}{dt^2} + \ell_{12}\frac{d^2\tilde{\phi}_1}{dt^2} + \ell_{13}\frac{d^2\tilde{\phi}_2}{dt^2} + \left(\ell_{14} + \ell_{15}\tilde{\phi}_1 + \ell_{16}\tilde{\phi}_2\right)\bar{w} \\
&\quad + \ell_{17}\tilde{\phi}_1 + \ell_{18}\tilde{\phi}_2 = 0
\end{aligned} \tag{13a}$$

$$-\ell_{21}\frac{d^2\tilde{w}}{dt^2} + \ell_{22}\frac{d^2\tilde{\phi}_1}{dt^2} + \ell_{23}\tilde{w} + \ell_{24}\tilde{\phi}_1 + \ell_{25}\tilde{\phi}_2 = 0 \tag{13b}$$

$$-\ell_{31}\frac{d^2\tilde{w}}{dt^2} + \ell_{32}\frac{d^2\tilde{\phi}_1}{dt^2} + \ell_{33}\tilde{w} + \ell_{34}\tilde{\phi}_1 + \ell_{35}\tilde{\phi}_2 = 0 \tag{13c}$$

in which the coefficients $\ell_{1i}(i = 1,2,..,8)$, $\ell_{ij}(i = 2,3; j = 1,2,.,5)$may be found in Appendix B. The inertial forces caused by the rotation angles $\tilde{\phi}_1$,$\tilde{\phi}_2$ are small so they can be ignored (i.e. $\ell_{12} = \ell_{13} = \ell_{21} = \ell_{22} = \ell_{31} = \ell_{32} = 0$) for Eqs. (13a), (13b), (13c). Eqs. (13a), (13b), (13c) can be rewritten as

$$\ell_{11}\frac{d^2\tilde{w}}{dt^2}+\left(\ell_{14}+\ell_{15}\tilde{\phi}_1+\ell_{16}\tilde{\phi}_2\right)\tilde{w}+\ell_{17}\tilde{\phi}_1+\ell_{18}\tilde{\phi}_2=0 \quad (14a)$$

$$\ell_{23}\tilde{w}+\ell_{24}\tilde{\phi}_1+\ell_{25}\tilde{\phi}_2=0 \quad (14b)$$

$$\ell_{33}\tilde{w}+\ell_{34}\tilde{\phi}_1+\ell_{35}\tilde{\phi}_2=0 \quad (14c)$$

Solving the Eqs. (14b) and (14c) with respect to $\tilde{\phi}_1$ and $\tilde{\phi}_2$ then substituting the results into the Eq. (14a) yields

$$\ell_{11}\frac{d^2\tilde{w}}{dt^2}+\tilde{\ell}_1\tilde{w}=0 \quad (15)$$

where

$$\tilde{\ell}_1=\ell_{14}+\frac{(\ell_{25}\ell_{33}-\ell_{23}\ell_{35})}{\ell_{25}(\ell_{24}\ell_{35}-\ell_{25}\ell_{34})}[\ell_{17}\ell_{25}-\ell_{18}(\ell_{23}+\ell_{24})] \quad (16)$$

The natural frequencies of a porous orthotropic laminated composite plate can be determined based on the hyperbolical shear deformation theory as:

$$\omega_{free}^{sdt}=\sqrt{\frac{\tilde{\ell}_1}{\ell_{11}}} \quad (17)$$

The natural frequencies within the classical plate theory can be determined by ignoring the shear strains in the theoretical formulations as:

$$\omega_{free}^{cpt}=\sqrt{\frac{\ell_{14}}{\ell_{11}}} \quad (18)$$

The non-dimensional natural frequencies can be determined as:

$$\bar{\omega}_{free}^{g}=\omega_{free}^{g}\left[\frac{a^2}{h}\sqrt{\rho_0/El_{02}}\right], g: sdt, cpt \quad (19)$$

5. Results and Discussion

The author focuses on the natural frequencies of two-layered plates with two porosity distributions as sinus and cosine functions. The author considers classical plate theory and hyperbolic shear deformation theory for frequency analysis. Also, the sensitivity of frequencies to porosity distributions, shear deformation, orthotropy ratio, and geometric properties are analyzed.

5.1. Verification study

This section focuses on comparing and verifying the obtained equations with the results available in the literature. As a first comparison, the current study's natural frequencies are compared with those in Reddy and Phan (1985). The results are presented in Table 1. The material and geometric properties of the non-porous orthotropic laminated plate are as follows:

$El_{01}=40El_{02},\ Sh_{023}=0.5El_{02},\ Sh_{012}=Sh_{013}=0.6El_{02},\ \upsilon_{012}=0.25,\frac{a}{b}=1,\ k=0$

Table 1 illustrates that the present study's results are consistent with the literature.

Table 1. Dimensionless natural frequencies, $\bar{\omega}_{\text{free}}^{g}(g: sdt, cpt)$, of non-porous orthotropic laminated composite plates.

Reddy and Phan (1985)				
	$0^o/90^o/90^o/0^o$		$0^o/90^o$	
a/h	*cpt*	*sdt*	*cpt*	*sdt*
12.5	18.707	16.276	11.066	10.686
25	18.780	18.050	11.139	11.037
50	18.799	17.606	11.158	11.132
Present study				
a/h	*cpt*	*sdt*	*cpt*	*sdt*
12.5	18.793	16.141	11.249	10.852
25	18.867	18.063	11.294	11.190
50	18.885	18.673	11.305	11.279

In the second comparison, the orthotropy ratio-dependent natural frequencies of layered plates are compared with those in Fares and Zenkour (1999). Table 2 shows the obtained results. The material and geometric properties of the considered non-porous orthotropic laminate are as follows: $El_{01}/El_{02}=open, Sh_{023}=0.5El_{02}, Sh_{012}=Sh_{013}=0.6El_{02}, \upsilon_{012}=0.25, a/b=1, a/h=5, k=0$. Table 2 shows that the current study's results are in good agreement with the literature.

Table 2. Dimensionless natural frequencies, $\tilde{\omega}_{\text{free}}^{sdt}=\omega_{\text{free}}^{sdt}h\sqrt{\rho_0 El_{02}}$, of non-porous orthotropic laminated composite plates.

El_{01}/El_{02}	Fares and Zenkour (1999)	Present study
3	0.2576	0.2593
10	0.3229	0.3212
20	0.3670	0.3631
30	0.3920	0.3869

5.2. Natural frequency analysis

This section involves the natural frequencies of two-layered plates with two different porosity models within the classical plate and shear deformation theories. The considered material properties of two-layered plates are given by: $El_{01}=137.9GPa,\ El_{02}=8.96GPa,\ Sh_{012}=Sh_{013}=7.10GPa,\ Sh_{023}=6.21GPa,\ \upsilon_{012}=0.3, \rho_0=1450kg.m^{-3}$.

Table 3 shows the variation of natural frequencies of two-layered plates with/without porosity (pm_3/pm_1). The considered parameters for analysis are given as $a/h=10, a/b=0.5, m=n=1$ and $k=0.4, 0.6$ and 0.8. The dimensionless natural frequencies of the non-porous/porous two-layered plates increase with the rising El_{01}/El_{02} ratio. The dimensionless natural frequencies of the porous single- and $90^o/0^o$ -layered plates decrease depending on the increase in the k coefficient. At the same time, the $0^o/90^o$-layered plates' natural frequencies diminish in $El_{01}/El_{02}\leq 25$ and rise in $El_{01}/El_{02}>25$.

Table 3. Dimensionless natural frequencies, $\bar{\omega}^{g}_{\text{free}}(g: sdt, cpt)$, of pm_1 and pm_3 model orthotropic laminated composite plates versus orthotropy ratio for three different layer sequences.

		0^o				$0^o/90^o$				$90^o/0^o$			
		pm_1		pm_3		pm_1		pm_3		pm_1		pm_3	
k	El_{01}/El_{02}	*cpt*	*sdt*	*cpt*	*sdt*	*cpt*	*sdt*	*cpt*	*sdt*	*cpt*	*sdt*	*cpt*	*sdt*
0.4	5	7.001	6.782	6.663	6.474	4.951	4.876	4.719	4.656	4.951	4.876	4.836	4.763
	15	11.373	10.439	10.824	10.012	6.008	5.883	5.970	5.854	6.008	5.883	5.783	5.663
	25	14.480	12.655	13.781	12.186	6.854	6.675	6.977	6.801	6.854	6.675	6.483	6.320
	35	17.030	14.235	16.208	13.752	7.599	7.361	7.853	7.607	7.599	7.361	7.094	6.886
	45	19.245	15.443	18.316	14.960	8.274	7.974	8.639	8.317	8.274	7.974	7.649	7.394
0.6	5	7.001	6.782	6.214	6.061	4.951	4.876	4.481	4.428	4.951	4.876	4.591	4.527
	15	11.373	10.439	10.094	9.430	6.008	5.883	5.870	5.764	6.008	5.883	5.495	5.388
	25	14.480	12.655	12.852	11.536	6.854	6.675	6.970	6.800	6.854	6.675	6.116	5.973
	35	17.030	14.235	15.115	13.075	7.599	7.361	7.915	7.670	7.599	7.361	6.649	6.469
	45	19.245	15.443	17.081	14.277	8.274	7.974	8.757	8.430	8.274	7.974	7.130	6.913
0.8	5	7.001	6.782	5.522	5.415	4.951	4.876	4.146	4.106	4.951	4.876	4.133	4.085
	15	11.373	10.439	8.970	8.499	6.008	5.883	5.708	5.614	6.008	5.883	4.960	4.878
	25	14.480	12.655	11.421	10.477	6.854	6.675	6.911	6.749	6.854	6.675	5.474	5.366
	35	17.030	14.235	13.432	11.954	7.599	7.361	7.929	7.688	7.599	7.361	5.898	5.765
	45	19.245	15.443	15.179	13.129	8.274	7.974	8.828	8.500	8.274	7.974	6.276	6.119

The non-porous laminated plates' frequencies are more significant than the porous ones for single- and $90^o/0^o$-layered plates. In contrast, they are less than the porous ones for $0^o/90^o$-layered plates in $El_{01}/El_{02} > 15$. With a rising orthotropy ratio, the natural frequency value difference between porous and non-porous laminated plates increases for single- and $90^o/0^o$-layered plates. It first decreases and then increases for $0^o/90^o$-layered plates. It rises depending on the increase in the k coefficient for all layer sequences. The non-porous/porous two-layered plates' natural frequencies are less than that of the non-porous/porous single-layered plates. The difference in natural frequency value between non-porous/porous single- and two-layered plates increases due to the rise of the orthotropy ratio. It diminishes with increasing the k coefficient. Suppose fiber orientation angles of two-layered plates are compared. In that case, the natural frequency values of non-porous two-layered plates are the same. However, the porous $0^o/90^o$-layered plates' natural frequency values are more significant than those of the porous $90^o/0^o$-layered plates in $El_{01}/El_{02} > 5$. The natural frequency value difference between porous two-layered plates increases with a rising in orthotropy ratio and k coefficient.

The influence of shear deformation on the natural frequencies of non-porous/porous laminated plates increases with a rising in the orthotropy ratio. With increasing El_{01}/El_{02} ratio from 5 to 45 at $k = 0.4$, the shear deformation effect on the natural frequencies of porous $0^o/90^o$ -layered plates rises from (1.3%) to (3.7%). The effect of shear deformation on the porous laminated plates' natural frequencies diminishes with an increase in porosity coefficient. The shear deformation effect on the natural frequencies of porous single-layered plates decreases from (18.3%) to (13.5%) with rising k from 0.4 to 0.8 at $El_{01}/El_{02} = 45$. The shear deformation effect on the natural frequencies of porous laminated plates is less than those of non-porous laminated plates. The shear deformation effect difference between the non-porous and porous two-layered plates is less than (1%) for increasing k and El_{01}/El_{02}. In contrast, the shear deformation effect difference between the non-porous and porous single-layered plates increases with rising k and El_{01}/El_{02}. It increases from (1.4%) to (6.3%) depending on the rise in k from 0.4 to 0.8 at $El_{01}/El_{02} = 45$. The shear deformation effect on the natural frequencies of non-porous/porous single-layered plates is more significant than two-layered plates' frequencies. The difference in shear deformation effect between non-porous single- and two-layered plates increases (15%) with increasing El_{01}/El_{02} from 5 to 45. The shear deformation effect difference between porous single- and two-layered plates decreases depending on the increase of k. With rising in k from 0.4 to 0.8 at $El_{01}/El_{02} = 45$, it diminishes from (14.6%) to (9.8%) for $0^o/90^o$-layer sequence. If fiber orientation angles of two-layered plates are compared, the shear deformation effect on the natural frequency of non-porous two-layered plates is the same. At the same time, the influence of shear deformation on the porous $90^o/0^o$ -layered plates' natural frequency is less than those of the porous $0^o/90^o$-layered plates in the range of $El_{01}/El_{02} > 15$. The shear deformation effect difference between porous two-layered plates increases with a rising k. This increase is less than (1%).

Due to the increase in the El_{01}/El_{02} ratio, the effect of the porosity model on the natural frequencies of porous single-layered plates diminishes for sdt and remains constant for cpt. At the same time, the porosity model effect on the natural frequencies increases for $90^o/0^o$, while it first decreases and then rises for $0^o/90^o$. With rising El_{01}/El_{02} from 5 to 45 at $k = 0.8$, the effect of the porosity model on the porous $0^o/90^o$-layered plates' natural frequencies diminishes first (11%) and then increases (6%).

The influence of the porosity model on the natural frequencies of porous laminated plates rises with increasing k coefficient for all layer sequences. The porosity model effect on the natural frequencies of $90^o/0^o$-layered plates increases (17%) with rising k from 0.4 to 0.8 when $El_{01}/El_{02} = 45$. The influence of the porosity model on the single-layered plates' natural frequencies is more significant than that of the $0^o/90^o$-layered plates. However, it is less than that of the $90^o/0^o$-layered plates in the range of $El_{01}/El_{02} > 25$. Due to the rise in the El_{01}/El_{02} ratio, the difference in the porosity model effect between the porous single- and two-layered plates increases first and then diminishes for the $0^o/90^o$-layer sequence. On the contrary, it decreases first and then rises for the $90^o/0^o$-layer sequence. Depending on the increase in El_{01}/El_{02} from 5 to 45 at $k = 0.8$ for sdt, the porosity model effect difference between the single- and $90^o/0^o$-layered plates diminishes first by (2.5%) and then rises by (6.8%).

The difference in the porosity model effect between the porous single- and two-layered plates increases with the rising k coefficient. The porosity model effect difference between the single- and $0^o/90^o$-layered plates increases from (1.8%) to (16.1%) with rising k from 0.4 to 0.8 at $El_{01}/El_{02} = 25$ for sdt. When two-layered plates' fiber orientation angles are compared, the influence of the porosity model on the natural frequencies of porous $0^o/90^o$-layered plates is less than that of $90^o/0^o$-layered plates in the range of $El_{01}/El_{02} > 5$. The porosity model effect difference between porous two-layered plates increases with a rise in k in the range of $El_{01}/El_{02} > 5$. It rises around (14%) for cpt and sdt due to the increase of k from 0.4 to 0.8 at $El_{01}/El_{02} = 45$. The difference in porosity model effect between porous two-layered plates rises first and then diminishes depending on the increase in the El_{01}/El_{02} ratio. It increases first by (19%) and then decreases by (2%) depending on the rise of El_{01}/El_{02} from 5 to 45 at $k = 0.8$ for sdt.

Fig. 3 presents the variation of natural frequencies of non-porous/porous two-layered plates. The selected parameters for analysis are given as $a/h = 10, m = n = 1$ and $k = 0.4, 0.6, 0.8$. The non-dimensional natural frequencies of the two-layered plates with/without porosity (pm_2/pm_1) rise with the increasing aspect ratio (a/b). The dimensionless natural frequencies of the porous single- and two-layered plates increase depending on the increase in the k coefficient. The porous laminated plates' natural frequencies are more significant than non-porous laminated plate ones. The natural frequency value difference between non-porous and porous laminated plates increases with the rise in aspect ratio and porosity coefficient for single-layered plates. It increases with increasing aspect ratio and porosity coefficient in the range of $a/b < 2.75$ for two-layered plates. The natural frequencies of non-porous/porous two-layered plates are less than those of non-porous/porous single-layered plates in $a/b < 1.75$. The natural frequency value difference between the single- and two-layered plates firstly diminishes and then increases with the rising aspect ratio. It increases depending on the rise of the porosity coefficient.

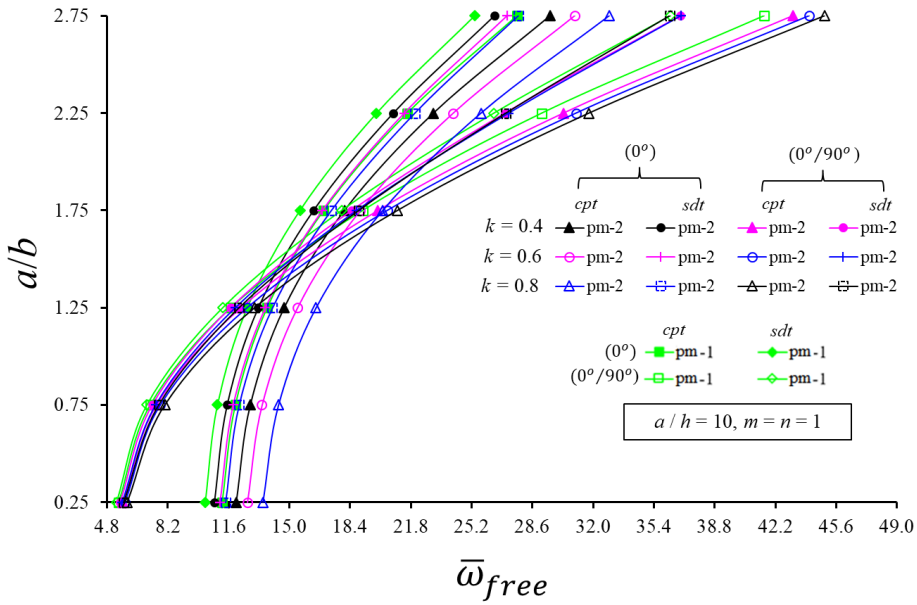

Fig. 3. Variation of the natural frequencies of porous orthotropic two-layered plate versus a/b and k for three different layer sequences.

Due to an increase in aspect ratio, the influence of shear deformation on the natural frequencies rises for two-layered plates. At the same time, it decreases first and then increases for single-layered plates. The shear deformation effect on the natural frequencies of non-porous two-layered plates increases by (11%) depending on the rise in a/b from 0.25 to 2.75. The effect of shear deformation on natural frequencies of porous two-layered plates rises with an increasing porosity coefficient. The shear deformation effect on the porous two-layered plates' natural frequencies increases from (14.6%) to (19.3%) with the rise in k from 0.4 to 0.8 at $a/b = 2.75$. The influence of shear deformation on the non-porous/porous single-layered plates' natural frequencies is more significant than that of non-porous/porous two-layered plates in $a/b < 2.25$. The difference in shear deformation effect between the non-porous/porous single- and two-layered plates firstly diminishes and then rises with increasing aspect ratio. The shear deformation effect difference between the non-porous single- and two-layered plates firstly decreases by (5%) and then increases by (2.7%) due to a rise in a/b from 0.25 to 2.75. The difference in shear deformation effect between the porous single- and two-layered plates increases with rising porosity coefficient (for $a/b < 2.25$). The shear deformation effect difference between the porous single- and two-layered plates rises from (7.9%) to (12.1%) with a rise in k from 0.4 to 0.8.

Depending on the increase in aspect ratio, the porosity model effect on the natural frequencies of porous laminated plates firstly increases and then decreases for two-layered plates. At the same time, it diminishes for single-layered plates. With rising a/b from 0.25 to 2.75 at $k = 0.8$ for sdt, the influence of the porosity model on the natural frequencies of porous two-layered plates firstly increases by (2%) and then decreases by (9.3%). The effect of the porosity model on the natural frequencies of porous laminated plates increases with the rise in the k coefficient. With increasing k from 0.4 to 0.8 at $a/b = 0.25$, the porosity model effect on the natural frequencies of porous single-layered plates rises (13%) and (6%) for cpt and sdt, respectively. The porosity model effect on the natural frequencies of porous two-layered plates is less than that of porous single-layered. The difference in porosity model effect between the porous single- and two-layered plates increases first and then decreases with increasing aspect ratio. Due to the rise in a/b from 0.25 to 2.75 at $k = 0.8$, the porosity model effect difference between the porous single- and two-layered plates firstly increases by (1.9%) and then decreases by (2.2%) for cpt. At the same time, it rises first (2%) and then diminishes (8.2%) for sdt. The difference in the porosity model effect between the porous single- and two-layered plates increases with the rising k. The porosity model effect difference between the porous single- and two-layered plates increases around (9%) with an increase in k from 0.4 to 0.8 at $a/b = 2.75$.

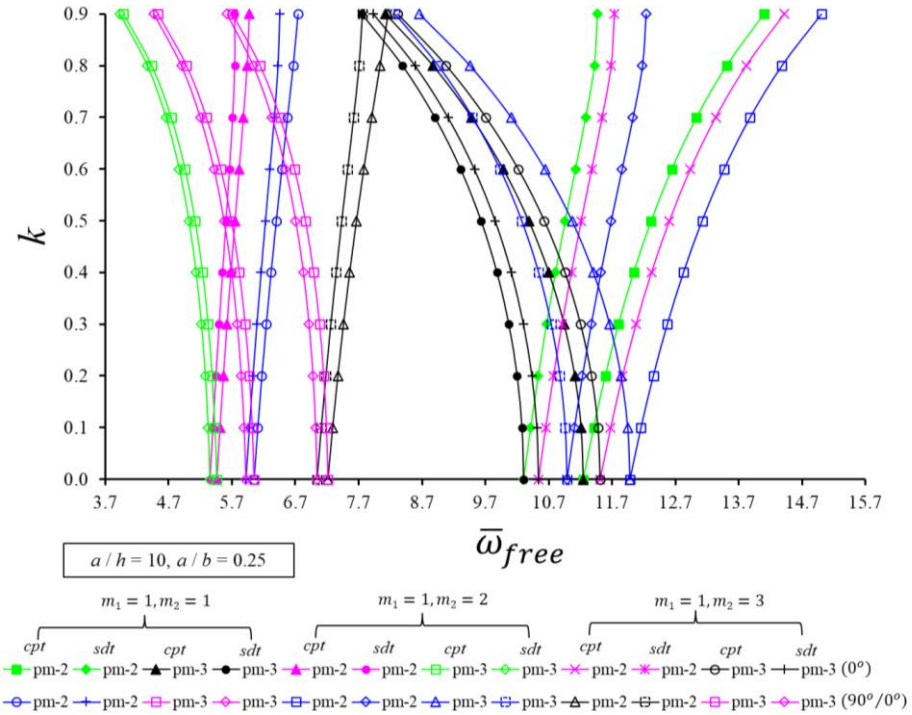

Fig. 4. Variation of the natural frequencies of porous orthotropic two-layered plate versus k and m_2 for different porosity models.

Fig. 4 illustrates the variation of natural frequencies of porous laminated plates depending on the k coefficient and wavenumbers. The considered parameters for analysis are given by $a/h = 10, a/b = 0.25$ and $m_2 = 1, 2, 3$. The dimensionless natural frequencies of the porous laminated plates increase for the pm_2 model and decrease for the pm_3 model with a rising k coefficient. The porous laminated plates' non-dimensional natural frequencies increase due to the rise in wavenumbers. The pm_3 model single- and two-layered plates' natural

frequencies are less than those of the pm_2 model ones in $k > 0$. The natural frequency value difference between the pm_2 and pm_3 models laminated plates rises with increasing k and m_2. The natural frequencies of porous single-layered plates are more significant than those of two-layered ones. Due to the rise in the k coefficient, the difference in natural frequency value between single- and two-layered plates diminishes for the pm_3 model and increases for the pm_2 model. At the same time, it decreases for pm_2 and pm_3 models with increasing m_2.

Depending on the rise in the k coefficient, the effect of shear deformation on the porous laminated plates' natural frequencies increases for the pm_2 model and decreases for the pm_3 model. Due to increasing k from 0 to 0.9 at $m_2 = 3$, the variations of shear deformation effect on single-layered plates' frequencies are (10%) and (4%) for pm_2 and pm_3 models, respectively. With increasing m_2, the influence of shear deformation on the natural frequencies of porous laminated plates diminishes for porous single-layered plates and rises for porous two-layered plates. The variations of shear deformation effect on two-layered plates' frequencies are less than (1.5%) depending on the rising m_2 from 1 to 3. The shear deformation effect on the pm_3 model laminated plates' natural frequencies is less than that of the pm_2 model ones. The difference in shear deformation effect between the pm_2 and pm_3 model laminated plates is more significant for porous single-layered plates. The shear deformation effect difference between the pm_2 and pm_3 model laminated plates increases with the rising k coefficient. Due to increasing k from 0 to 0.9 at $m_2 = 3$, it rises (14%) and (3.5%) for single- and two-layered plates, respectively. Depending on the increasing m_2, the difference in shear deformation effect between the pm_2 and pm_3 model laminated plates decreases for single-layered plates and rises for two-layered plates. The difference variation is around (1%) for both porous laminated plates due to the rise in m_2 from 1 to 3 at $k = 0.9$. The influence of shear deformation on the natural frequencies of the porous single-layered plates is more significant than those of porous two-layered plates. The shear deformation effect difference between the porous single- and two-layered plates decreases with increasing m_2. At the same time, it diminishes for pm_3 model and rises for pm_2 model with rising k. It rises from (6%) to (14%) depending on the increase in k from 0 to 0.9 at $m_2 = 3$. Also, its variation is less than (1.5%) depending on the rising m_2 from 1 to 3 at $k = 0.9$.

The effect of the porosity model on the porous laminated plates' natural frequencies increases depending on the rise in the k coefficient. With increasing k from 0 to 0.9 at $m_2 = 2$ for single-layered plates in sdt, it rises (11.3%) and (24.8%) for pm_2 and pm_3 models, respectively. The porosity model effect on natural frequencies of porous laminated plates decreases with rising m_2 for single-layered plates. At the same time, it increases for the pm_2 model and diminishes for pm_3 with increasing m_2 in two-layered plates. With rising m_2 from 1 to 3 at $k = 0.9$ for porous two-layered plates in sdt, the porosity model effect increases by (2.8%) and decreases by (6.3%) for the pm_2 and pm_3 models, respectively. The pm_3 model effect on the laminated plates' natural frequencies is more significant than the pm_2 model ones in the range of $k > 0.4$ for sdt. The porosity model effect difference between the pm_2 and pm_3 models increases for rising k and decreases for increasing m_2. The difference in the porosity model effect between the pm_2 and pm_3 model two-layered plates increases (15.4%) with rising k from 0 to 0.9 at $m_2 = 2$ for sdt. It diminishes (9.1%) with rising m_2 from 1 to 3 at $k = 0.9$ for sdt. The pm_2 model effect on the porous single-layered plates' natural frequencies is more significant than that of two-layered ones. However, the pm_3 model effect on the porous single-layered plates' natural frequencies is less than that of two-layered ones in $k < 0.4$ and $k < 0.5$ for cpt and sdt, respectively. The difference in the porosity model effect between the porous single- and two-layered plates increases with rising k. At the same time, it diminishes for the pm_2 model and increases for the pm_3 model with the rise in m_2. With rising k from 0 to 0.9 at $m_2 = 3$ for sdt, the porosity model effect difference between the single- and two-layered plates increases (1.3%) and (4.5%) for pm_2 and pm_3 models, respectively. Its variation depending on the increase in m_2 from 1 to 3 at $k = 0.9$ for sdt is (2.8%) in pm_2 and pm_3 models.

6. Conclusions

Porous materials, widely used to reduce structural weight and manage vibration responses, and laminated composites, used in the aircraft and aerospace industries due to their superior properties, are combined in this study. The effects of this combination on the free vibration response of the porous laminated plates were emphasized by comparing them with the classical or non-porous laminated plates. This paper analyzes the natural frequencies of two-layered composite plates with two different porosity distributions within the higher-order shear deformation theory. The influences of porosity models, shear deformation, and geometric parameters on porous two-layered composite plates are discussed in detail. The notable results are as follows:

- The dimensionless natural frequencies of the pm_3 model single- and $90^o/0^o$ -layered plates decrease with the rising k coefficient. The non-dimensional natural frequencies of the pm_2 model $0^o/90^o$ - and $90^o/0^o$-layered plates increase with increasing k coefficient.
- The natural frequencies of non-porous $0^o/90^o$ -layered plates are less than those of the porous ones, and the non-porous $90^o/0^o$ -layered plates' natural frequencies are more significant than those of the porous ones.
- The pm_3 model laminated plates' natural frequencies are less than those of the pm_2 model ones.
- The influence of shear deformation on the natural frequencies of porous two-layered plates increases for the pm_2 model and decreases for the pm_3 model depending on the rise in the k coefficient.
- The shear deformation effect on the natural frequencies of porous laminated plates is less than those of non-porous ones.

- The shear deformation effect on the natural frequencies of porous single-layered plates is more significant than two-layered plates' frequencies.
- The shear deformation effect on the pm_3 model laminated plates' natural frequencies is less than that of the pm_2 model ones.
- The porosity model effect on the natural frequencies of porous two-layered plates rises with increasing k coefficient.
- The pm_2 and pm_3 (for $k > 0.4$) model effect on the porous single-layered plates' natural frequencies is more significant than that of $0^o/90^o$-layered ones for sdt.

Appendix A.

$$\Im_{11}^0 = \tilde{d}_{11}^1\tau_{11}^0 + \tilde{d}_{12}^1\tau_{21}^0, \Im_{12}^0 = \tilde{d}_{11}^1\tau_{12}^0 + \tilde{d}_{12}^1\tau_{22}^0, \Im_{21}^0 = \tilde{d}_{21}^1\tau_{11}^0 + \tilde{d}_{22}^1\tau_{21}^0, \Im_{22}^0 = \tilde{d}_{21}^1\tau_{12}^0 + \tilde{d}_{22}^1\tau_{22}^0,$$

$$\Im_{11}^1 = \tilde{d}_{11}^1\tau_{11}^1 + \tilde{d}_{12}^1\tau_{21}^1 - \tilde{d}_{11}^2, \Im_{12}^1 = \tilde{d}_{11}^1\tau_{12}^1 + \tilde{d}_{12}^1\tau_{22}^1 - \tilde{d}_{12}^2, \Im_{21}^1 = \tilde{d}_{21}^1\tau_{11}^1 + \tilde{d}_{22}^1\tau_{21}^1 - \tilde{d}_{21}^2,$$

$$\Im_{22}^1 = \tilde{d}_{21}^1\tau_{12}^1 + \tilde{d}_{22}^1\tau_{22}^1 - \tilde{d}_{22}^2, \Im_{11}^2 = \tilde{d}_{11}^1\tau_{11}^3 + \tilde{d}_{12}^1\tau_{21}^3 + \tilde{d}_{11}^4, \Im_{12}^2 = \tilde{d}_{11}^1\tau_{12}^3 + \tilde{d}_{12}^1\tau_{22}^3 + \tilde{d}_{12}^4,$$

$$\Im_{21}^2 = \tilde{d}_{21}^1\tau_{11}^3 + \tilde{d}_{22}^1\tau_{21}^3 + \tilde{d}_{21}^4, \Im_{22}^2 = \tilde{d}_{21}^1\tau_{12}^3 + \tilde{d}_{22}^1\tau_{22}^3 + \tilde{d}_{22}^4, \Im_{11}^3 = \tilde{d}_{11}^3\tau_{11}^0 + \tilde{d}_{12}^3\tau_{21}^0,$$

$$\Im_{12}^3 = \tilde{d}_{11}^3\tau_{12}^0 + \tilde{d}_{12}^3\tau_{22}^0, \Im_{21}^3 = \tilde{d}_{21}^3\tau_{11}^0 + \tilde{d}_{22}^3\tau_{21}^0, \Im_{22}^3 = \tilde{d}_{21}^3\tau_{12}^0 + \tilde{d}_{22}^3\tau_{22}^0, \Im_{11}^4 = \tilde{d}_{11}^3\tau_{11}^1 + \tilde{d}_{12}^3\tau_{21}^1 - \tilde{d}_{11}^4,$$

$$\Im_{12}^4 = \tilde{d}_{11}^3\tau_{12}^1 + \tilde{d}_{12}^3\tau_{22}^1 - \tilde{d}_{12}^4, \Im_{21}^4 = \tilde{d}_{21}^3\tau_{11}^1 + \tilde{d}_{22}^3\tau_{21}^1 - \tilde{d}_{21}^4, \Im_{22}^4 = \tilde{d}_{21}^3\tau_{12}^1 + \tilde{d}_{22}^3\tau_{22}^1 - \tilde{d}_{22}^4,$$

$$\Im_{11}^5 = \tilde{d}_{11}^3\tau_{11}^3 + \tilde{d}_{12}^3\tau_{21}^3 + \tilde{d}_{11}^5, \Im_{12}^5 = \tilde{d}_{11}^3\tau_{12}^3 + \tilde{d}_{12}^3\tau_{22}^3 + \tilde{d}_{12}^5, \Im_{21}^5 = \tilde{d}_{21}^3\tau_{11}^3 + \tilde{d}_{22}^3\tau_{21}^3 + \tilde{d}_{21}^5,$$

$$\Im_{22}^5 = \tilde{d}_{21}^3\tau_{12}^3 + \tilde{d}_{22}^3\tau_{22}^3 + \tilde{d}_{22}^5, \Im_{66}^0 = \tilde{d}_{66}^1\tau_{66}^0, \Im_{66}^1 = \tilde{d}_{66}^1\tau_{66}^1 - 2\tilde{d}_{66}^2, \Im_{66}^2 = \tilde{d}_{66}^1\tau_{66}^3 + \tilde{d}_{66}^4, \Im_{66}^3 = \tilde{d}_{66}^3\tau_{66}^0,$$

$$\Im_{66}^4 = \tilde{d}_{66}^3\tau_{66}^1 - 2\tilde{d}_{66}^4, \Im_{66}^5 = \tilde{d}_{66}^3\tau_{66}^3 + \tilde{d}_{66}^5 \quad \text{(A1)}$$

with

$$\tau_{11}^0 = \frac{\tilde{d}_{22}^0}{\tilde{\Delta}}, \tau_{12}^0 = \frac{-\tilde{d}_{12}^0}{\tilde{\Delta}}, \tau_{21}^0 = \frac{-\tilde{d}_{21}^0}{\tilde{\Delta}}, \tau_{22}^0 = \frac{\tilde{d}_{11}^0}{\tilde{\Delta}},$$

$$\tau_{11}^1 = \frac{\tilde{d}_{22}^0\tilde{d}_{11}^1 - \tilde{d}_{12}^0\tilde{d}_{21}^1}{\tilde{\Delta}}, \tau_{12}^1 = \frac{\tilde{d}_{22}^0\tilde{d}_{12}^1 - \tilde{d}_{12}^0\tilde{d}_{22}^1}{\tilde{\Delta}},$$

$$\tau_{21}^1 = \frac{\tilde{d}_{11}^0\tilde{d}_{21}^1 - \tilde{d}_{21}^0\tilde{d}_{11}^1}{\tilde{\Delta}}, \tau_{22}^1 = \frac{\tilde{d}_{11}^0\tilde{d}_{22}^1 - \tilde{d}_{21}^0\tilde{d}_{12}^1}{\tilde{\Delta}},$$

$$\tau_{11}^3 = \frac{\tilde{d}_{12}^0\tilde{d}_{21}^3 - \tilde{d}_{22}^0\tilde{d}_{11}^3}{\tilde{\Delta}}, \tau_{12}^3 = \frac{\tilde{d}_{12}^0\tilde{d}_{22}^3 - \tilde{d}_{22}^0\tilde{d}_{12}^3}{\tilde{\Delta}},$$

$$\tau_{21}^3 = \frac{\tilde{d}_{21}^0\tilde{d}_{11}^3 - \tilde{d}_{11}^0\tilde{d}_{21}^3}{\tilde{\Delta}}, \tau_{22}^3 = \frac{\tilde{d}_{21}^0\tilde{d}_{12}^3 - \tilde{d}_{11}^0\tilde{d}_{22}^3}{\tilde{\Delta}},$$

$$\tau_{66}^0 = \frac{1}{\tilde{d}_{66}^0}, \tau_{66}^1 = \frac{2\tilde{d}_{66}^1}{\tilde{d}_{66}^0}, \tau_{66}^3 = \frac{-\tilde{d}_{66}^3}{\tilde{d}_{66}^0}, \tilde{\Delta} = \tilde{d}_{11}^0\tilde{d}_{22}^0 - \tilde{d}_{12}^0\tilde{d}_{21}^0,$$

$$\tilde{d}_{ij}^{\ell} = \sum_{n=1}^{N}\int_{\bar{z}_{n-1}}^{\bar{z}_n}(\bar{z})^{\ell}d_{ij}^{(n)}d\bar{z},$$

$$\tilde{d}_{ij}^{\ell+3} = \sum_{n=1}^{N}\int_{\bar{z}_{n-1}}^{\bar{z}_n}(\bar{z})^{2\ell-\ell^2}\varphi(\bar{z})^{0.5(\ell^2-\ell+2)}d_{ij}^{(n)}d\bar{z}, i,j = 1,2,6; \ell = 0,1,2,$$

$$\tilde{d}_{ij}^0 = \sum_{n=1}^{N}\int_{\bar{z}_{n-1}}^{\bar{z}_n}\left(\frac{d\varphi(\bar{z})}{d\bar{z}}\right)^2 d_{ij}^{(n)}d\bar{z}, i,j = 4,5 \quad \text{(A2)}$$

with

$$\bar{\iota}_1 = \frac{\iota_1^2}{\iota_0} - \iota_2, \bar{\iota}_2 = \iota_4 - \frac{\iota_1\iota_3}{\iota_0}, \bar{\iota}_3 = \iota_5 - \frac{\iota_3^2}{\iota_0},$$

$$(\iota_0, \iota_1, \iota_2, \iota_3, \iota_4, \iota_5) = \sum_{n=1}^{N}\int_{\bar{z}_{n-1}}^{\bar{z}_n}\rho(\bar{z})(1, \bar{z}, \bar{z}^2, \varphi(\bar{z}), \bar{z}\varphi(\bar{z}), \varphi(\bar{z})^2)d\bar{z} \quad \text{(A3)}$$

Appendix B.

$$\ell_{11} = \frac{ab(\bar{\iota}_1(\eta_1^2+\eta_2^2)-\iota_0)}{4}, \ \ell_{12} = \frac{ab\eta_1\bar{\iota}_2}{4}, \ \ell_{13} = \frac{ab\eta_2\bar{\iota}_2}{4},$$

$$\ell_{14} = \frac{ab}{4}[\eta_1^4(r_4 + r_3\beta_1) + \eta_1^2\eta_2^2(r_5 + r_1\beta_1) + \eta_2^4(r_6 + r_2\beta_1)],$$

$$\ell_{15} = \frac{8\eta_1\eta_2\beta_2}{3}, \ \ell_{16} = \frac{8\eta_1\eta_2\beta_3}{3},$$

$$\ell_{17} = \frac{ab}{4}[(\eta_1^4 r_3 + \eta_1^2\eta_2^2 r_1 + \eta_2^4 r_2)\beta_2 + \eta_1(\eta_1^2 r_7 + \eta_2^2 r_8)],$$

$$\ell_{18} = \frac{ab}{4}[(\eta_1^4 r_3 + \eta_1^2\eta_2^2 r_1 + \eta_2^4 r_2)\beta_3 + \eta_2(\eta_1^2 r_9 + \eta_2^2 r_{10}),$$

$$\ell_{21} = \eta_1^2\bar{\iota}_2\frac{ab}{4}, \ \ell_{22} = \eta_1\bar{\iota}_3\frac{ab}{4},$$

$$\ell_{23} = \frac{ab}{4}[\eta_1^4(r_{13} + r_{12}\beta_1) + \eta_1^2\eta_2^2(r_{14} + r_{11}\beta_1)],$$

$$\ell_{24} = \frac{ab}{4}[(\eta_1^4 r_{12} + \eta_1^2\eta_2^2 r_{11})\beta_2 + \eta_1(\eta_1^2 r_{15} + \eta_2^2 r_{16} + r_{18})],$$

$$\ell_{25} = \frac{ab}{4}[(\eta_1^4 r_{12} + \eta_1^2\eta_2^2 r_{11})\beta_3 + \eta_1^2\eta_2 r_{17}],$$

$$\ell_{31} = \eta_2^2\bar{\iota}_2\frac{ab}{4}, \ \ell_{32} = \eta_2\bar{\iota}_3\frac{ab}{4},$$

$$\ell_{33} = \frac{ab}{4}[\eta_1^2\eta_2^2(r_{21} + r_{20}\beta_1) + \eta_2^4(r_{22} + r_{19}\beta_1)],$$

$$\ell_{34} = \frac{ab}{4}[(\eta_1^2\eta_2^2 r_{20} + \eta_2^4 r_{19})\beta_2 + \eta_1\eta_2^2 r_{23}],$$

$$\ell_{35} = \frac{ab}{4}[(\eta_1^2\eta_2^2 r_{20} + \eta_2^4 r_{19})\beta_3 + \eta_2(\eta_1^2 r_{25} + \eta_2^2 r_{24} + r_{26})] \quad \text{(B1)}$$

with

$$r_1 = \Im_{11}^0 + \Im_{22}^0 - 2\Im_{66}^0, \ r_2 = \Im_{21}^0, \ r_3 = \Im_{12}^0, \ r_4 = \Im_{11}^1,$$

$$r_5 = \mathfrak{I}_{12}^1 + \mathfrak{I}_{21}^1 + 2\mathfrak{I}_{66}^1,\ r_6 = \mathfrak{I}_{22}^1,\ r_7 = \mathfrak{I}_{11}^2,$$

$$r_8 = \mathfrak{I}_{21}^2 + 2\mathfrak{I}_{66}^2,\ r_9 = \mathfrak{I}_{12}^2 + 2\mathfrak{I}_{66}^2,$$

$$r_{10} = \mathfrak{I}_{22}^2,\ r_{11} = \mathfrak{I}_{11}^3 - \mathfrak{I}_{66}^3,\ r_{12} = \mathfrak{I}_{12}^3,\ r_{13} = \mathfrak{I}_{11}^4,$$

$$r_{14} = \mathfrak{I}_{12}^4 + \mathfrak{I}_{66}^4,\ r_{15} = \mathfrak{I}_{11}^5,\ r_{16} = \mathfrak{I}_{66}^5,\ r_{17} = \mathfrak{I}_{12}^5 + \mathfrak{I}_{66}^5,$$

$$r_{18} = \tilde{d}_{55}^0,\ r_{19} = \mathfrak{I}_{21}^3,\ r_{20} = \mathfrak{I}_{22}^3 - \mathfrak{I}_{66}^3,\ r_{21} = \mathfrak{I}_{21}^4 + \mathfrak{I}_{66}^4,$$

$$r_{22} = \mathfrak{I}_{22}^4,\ r_{23} = \mathfrak{I}_{21}^5 + \mathfrak{I}_{66}^5,\ r_{24} = \mathfrak{I}_{22}^5,$$

$$r_{25} = \mathfrak{I}_{66}^5,\ r_{26} = \tilde{d}_{44}^0 \qquad \text{(B2)}$$

Acknowledgements

None declared.

Funding

The author received no financial support for the research, authorship, and/or publication of this manuscript.

Conflict of Interest

The author declared no potential conflicts of interest with respect to the research, authorship, and/or publication of this manuscript.

References

Arshid E, Amir S, Loghman A (2020). Static and dynamic analyses of FG-GNPs reinforced porous nanocomposite annular micro-plates based on MSGT. *International Journal of Mechanical Sciences*, 180, 105656.

Aydogdu M (2009). A new shear deformation theory for laminated composite plates. *Composite Structures*, 89(1), 94-101.

Chen Z, Qin B, Zhong R, Wang Q (2022). Free in-plane vibration analysis of elastically restrained functionally graded porous plates with porosity distributions in the thickness and in-plane directions. *The European Physical Journal Plus*, 137(1), 1-21.

Esen I, Özmen R (2022). Thermal vibration and buckling of magneto-electro-elastic functionally graded porous nanoplates using nonlocal strain gradient elasticity. *Composite Structures*, 296, 115878.

Esmaeilzadeh M, Kadkhodayan M, Mohammadi S, Turvey GJ (2020). Nonlinear dynamic analysis of moving bilayer plates resting on elastic foundations. *Applied Mathematics and Mechanics (English Edition)*, 41(3), 439-458.

Fares M, Zenkour A (1999). Buckling and free vibration of non-homogeneous composite cross-ply laminated plates with various plate theories. *Composite Structures*, 44(4), 279-287.

Hung P, Phung-Van P, Thai CH (2022). A refined isogeometric plate analysis of porous metal foam microplates using modified strain gradient theory. *Composite Structures*, 289, 115467.

Kumar P, Harsha SP (2022). Static and vibration response analysis of sigmoid function-based functionally graded piezoelectric non-uniform porous plate. *Journal of Intelligent Material Systems and Structures*, 1045389X221077433.

Kumar Y, Gupta A, Tounsi A (2021). Size-dependent vibration response of porous graded nanostructure with FEM and nonlocal continuum model. *Advances in Nano Research*, 11(1), 1-17.

Lahdiri A, Kadri M (2022). Free vibration behaviour of multi-directional functionally graded imperfect plates using 3D isogeometric approach. *Earthquakes and Structures*, 22(5), 527-538.

Li S, Zheng S, Chen D (2020). Porosity-dependent isogeometric analysis of bi-directional functionally graded plates. *Thin-Walled Structures*, 156, 106999.

Mahi A, Adda Bedia EA, Tounsi A (2015). A new hyperbolic shear deformation theory for bending and free vibration analysis of isotropic, functionally graded, sandwich and laminated composite plates. *Applied Mathematical Modelling*, 39(9), 2489-2508.

Pan H-G, Wu Y-S, Zhou J-N, Fu Y-M, Liang X, Zhao T-Y (2021). Free vibration analysis of a graphene-reinforced porous composite plate with different boundary conditions. *Materials*, 14(14), 3879.

Pham Q-H, Nguyen P-C, Tran V-K, Nguyen-Thoi T (2021). Finite element analysis for functionally graded porous nano-plates resting on elastic foundation. *Steel and Composite Structures*, 41(2), 149-166.

Reddy JN, Phan ND (1985). Stability and vibration of isotropic, orthotropic and laminated plates according to a higher-order shear deformation theory. *Journal of Sound and Vibration*, 98(2), 157-170.

Safaei B, (2020). The effect of embedding a porous core on the free vibration behavior of laminated composite plates. *Steel and Composite Structures*, 35(5), 659-670.

Shi P, Dong C, Sun F, Liu W, Hu Q (2018). A new higher order shear deformation theory for static, vibration and buckling responses of laminated plates with the isogeometric analysis. *Composite Structures*, 204 342-358.

Teng Z, Xi P (2021). Analysis on free vibration and critical buckling load of a FGM porous rectangular plate. *Xibei Gongye Daxue Xuebao/Journal of Northwestern Polytechnical University*. 39(2), 317-325.

Turan F, Başoğlu MF, Zerin Z (2017). Analytical solution for bending and buckling response of laminated non-homogeneous plates using a simplified-higher order theory. *Challenge Journal of Structural Mechanics*, 3(1), 1-16.

Wang W, Xue G, Teng Z (2022). Analysis of free vibration characteristics of porous FGM circular plates in a temperature field. *Journal of Vibration Engineering & Technologies*, 1-12.

Xu K, Yuan Y, Li M (2019). Buckling behavior of functionally graded porous plates integrated with laminated composite faces sheets. *Steel and Composite Structures*, 32(5), 633-642.

Yuan Y, Zhao K, Xu K (2019). Enhancing the static behavior of laminated composite plates using a porous layer. *Structural Engineering and Mechanics*, 72(6), 763-774.

Zenkour AM, Radwan AF (2016). Free vibration analysis of multilayered composite and soft core sandwich plates resting on Winkler–Pasternak foundations. *Journal of Sandwich Structures & Materials*, 20(2), 169-190.

Zhong R, Qin B, Wang Q, Shao W, Shuai C (2021). Prediction of the in-plane vibration behavior of porous annular plate with porosity distributions in the thickness and radial directions. *Mechanics of Advanced Materials and Structures*, 1-25.

Zhou C, Zhan Z, Zhang J, Fang Y, Tahouneh V (2020). Vibration analysis of FG porous rectangular plates reinforced by graphene platelets. *Steel and Composite Structures*, 34(2), 215-226.